OAK RIDGE NATIONAL LABORATORY
operated by
UNION CARBIDE CORPORATION
for the
U.S. ATOMIC ENERGY COMMISSION

ORNL-TM-166

COLLAPSE OF TUBES BY EXTERNAL PRESSURE

C. R. KENNEDY
J. T. VENARD

NOTICE

ORNL-TM-166

Copy

Contract No. W-7405-eng-26

Metals and Ceramics Division

COLLAPSE OF TUBES BY EXTERNAL PRESSURE

C. R. Kennedy and J. T. Venard

DATE ISSUED

APR 17 1962

OAK RIDGE NATIONAL LABORATORY
Oak Ridge, Tennessee
operated by
UNION CARBIDE CORPORATION
for the
U. S. ATOMIC ENERGY COMMISSION

COLLAPSE OF TUBES BY EXTERNAL PRESSURE

C. R. Kennedy and J. T. Venard

ABSTRACT

The problem of tube collapse by external pressure has been investigated experimentally. A graphical solution developed to simplify inelastic collapse design problems was shown to agree with the test results. The von Karman reduced modulus was used in the graphical solution to correct for the stress redistribution caused by yielding. The effects of the geometric imperfections of ovality and wall-thickness variations on collapse pressure were shown to be related to the stress-strain behavior of the material. The concept of a "critical time" was discussed in regard to creep-buckling phenomenon.

INTRODUCTION

As a result of the interest in tube collapse by external pressure, dating from the first experiments of Fairbairn[1] in 1858, several theoretical and empirical solutions have been obtained. The code methods derived from these solutions in general contain safety factors of unknown magnitude which allow for geometric imperfections, material imperfections, and a confidence factor. The use of such code methods is overly restrictive under conditions where optimum design is required for efficient operation, particularly in reactor design at elevated temperatures, where neutron economy dictates a minimum mass in the flux field.

This investigation applies previous solutions for instantaneous collapse of perfect tubes to experimental results obtained at elevated temperatures. The effect of geometric imperfections in reducing the critical pressure for collapse was determined so that more appropriate safety factors could be used. The confidence factor is not discussed

---

[1]W. Fairbairn, Phil. Trans. Roy. Soc. London 148(A), 389–413 (1858).

since it must be determined independently for each design by balancing operating efficiency and initial cost against failure and replacement costs.

Time-dependent or creep collapse experiments have not yet been performed, but the problem is considered in view of its importance in design at the elevated temperatures.

EXPERIMENTAL PROCEDURE

Specimens

Tube specimens were fabricated from seamless type 304 stainless steel pipe and tubing to give radius to wall thickness ratios ranging from 10 to 25. These ratios were obtained by honing the inside diameter and grinding the outside diameter to closely held tolerances. The required range of ratios necessitated the use of several heats of material.

Deliberate wall-thickness variations of up to ±10% were produced by off-center grinding in a number of specimens. Specimens were also deformed in a press to obtain tubes of an oval shape. All specimens were annealed at 1900°F for 1 hr in hydrogen after machining and forming operations.

The finished and annealed specimens were provided with slip-fit end plugs welded with an edge fusion weld, with a resulting unsupported length of 11.0 in. in most cases. End defects required that two 0.025-in.-wall specimens be shortened to a 9.0-in. free length and two 0.015-in.-wall specimens to an 8.0-in. free length. A schematic drawing of a typical specimen showing end plugs and 1/4-in. vent tube is shown in Fig. 1.

Tensile data were obtained by pulling 3.0-in. sections of typical specimens fitted with special end plugs for gripping.

Capsule

The experimental capsule consisted of a length of 2-in. sched-40 Inconel pipe with welded pipe-cap end closures; a cutaway view is shown in Fig. 2. The top cap was drilled to receive the specimen vent tube,

UNCLASSIFIED
ORNL-LR-DWG 64882

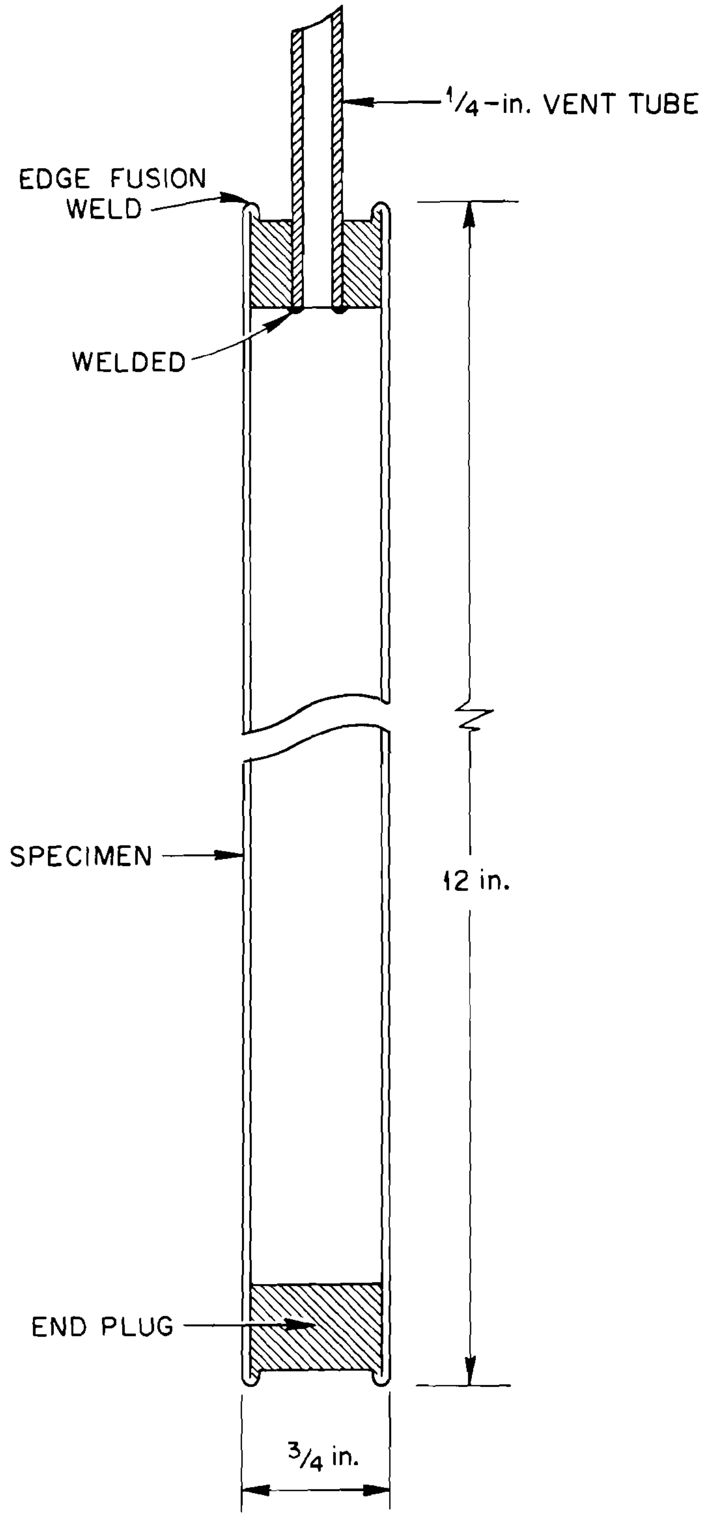

Fig. 1. Tube Collapse Specimen.

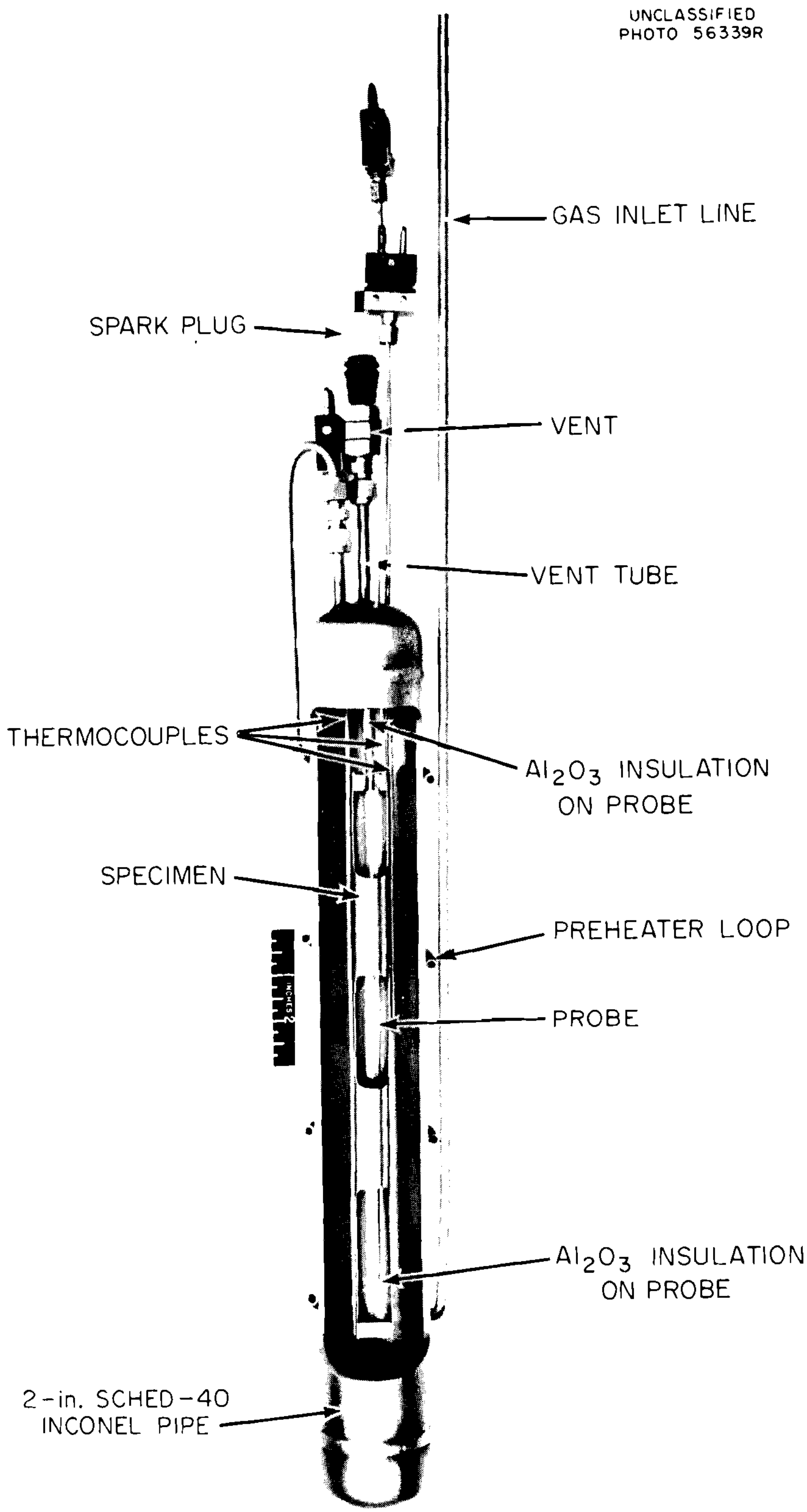

Fig. 2. Cutaway View of Tube Collapse Capsule.

three swaged thermocouples, and a pressure line. The top cap assembly was welded together and inserted into the capsule, and then the closure weld was made.

An inlet gas preheater loop around the outside of the capsule prevented the specimen from cooling during pressurization. Test temperatures, as determined by the top, middle, and bottom thermocouples, were maintained within ±9°F over the specimen length during the test.

The capsule was placed in a furnace and brought to 1200°F, the test temperature. When equilibrium was reached, the capsule was pressurized at approximately 300 psig of argon per minute until collapse occurred. The capsule pressure was recorded on a strip chart recorder reading the output of a strain-gage fluid-pressure cell. A relay system which was actuated by the probe shorting against the specimen wall and which simultaneously energized an event marker on the pressure time chart and a light on the control panel was initially used to indicate failure or specimen collapse. The probe system was abandoned, however, when it became evident that the discontinuity obtained on the pressure vs time recording plus the definite and quite audible snap of the collapse were sufficient indications of failure.

Time of test, maximum pressure, and loading rate for each test were obtained by examination of the pressure vs time chart.

EXPERIMENTAL RESULTS

The experimental results are tabulated in Table 1, which gives material identification, information on the specimen dimensions, collapsing pressure, and time of test. Stress-strain curves obtained for materials 23999X and 24555 are shown in Figs. 3 and 4, respectively. It is important to note the agreement between the two curves shown in Fig. 3 despite the strain rates differing by a factor of 30. Figure 5 presents some typical specimens after test. It was interesting to observe that specimens having wall-thickness variations of less than 5% exhibited a uniform two-lobe collapse, while those having 10 to 13% variations failed in a twisted and uneven manner along their length.

Table 1. Instantaneous Tube Collapse Data for Type 304 Stainless Steel at 1200°F
(All specimens annealed at 1900°F for 1 hr in hydrogen)

Test No.	Heat No.	Average Wall Thickness (in.)	Average Outside Diameter (in.)	Mean Radius / Average Wall Thickness	Wall-Thickness Variation (%)	Initial Deflection / Average Wall Thickness	Specimen Length (in.)	Collapse Pressure (psi)	Test Time (min)
638	23999X	0.01500	0.7520	24.57	3.33	0.02	9.0	320	1.0
639	23999X	0.01510	0.7520	24.40	4.64	0.02	9.0	310	1.0
663	23999X	0.01483	0.7518	24.85	5.39	0.03	12.0	360	1.5
664	23999X	0.01607	0.7518	22.89	13.50	0.01	12.0	330	1.0
613	McJunkin	0.02031	0.7402	17.72	4.97	< 0.01	12.0	540	0.5
614	McJunkin	0.02056	0.7402	17.50	3.70	< 0.01	12.0	560	3.5
630	23999X	0.02103	0.7528	17.40	1.78	0.01	12.0	660	2.0
659	23999X	0.02115	0.7529	17.30	1.65	0.01	12.0	660	2.0
615	24555	0.02510	0.7490	14.42	3.98	0.01	12.0	760	6.5
636	24555	0.02473	0.7490	14.64	3.23	0.01	10.0	780	3.0
637	24555	0.02505	0.7490	14.45	4.39	0.01	10.0	820	2.5
640	McJunkin	0.02509	0.7505	14.46	10.32	0.01	12.0	800	
655	24555	0.03100	0.7494	11.59	2.26	0.01	12.0	1040	4.0
656	24555	0.03100	0.7493	11.58	2.58	< 0.01	12.0	1090	3.5
621	24555	0.03323	0.7492	10.77	0.83	< 0.01	12.0	1200	4.0
622	24555	0.03305	0.7490	10.83	1.06	0.01	12.0	1150	5.0
631	24555	0.03325	1.0002	14.54	0.46	0.01	12.0	840	2.5
633	24555	0.03345	1.0001	14.45	0.45	< 0.01	12.0	860	2.5
652	24555	0.02585	0.7521	14.05	1.35	0.89	12.0	160	0.5
654	24555	0.02570	0.7518	14.13	2.62	0.88	12.0	160	0.5
661	24555	0.02560	0.7520	14.19	2.34	0.26	12.0	360	1.0
662	24555	0.02580	0.7519	14.07	1.16	0.27	12.0	430	1.5
667	24555	0.02585	0.7518	14.04	1.74	0.14	12.0	360	1.5
668	24555	0.02600	0.7520	13.96	1.92	0.14	12.0	440	1.5

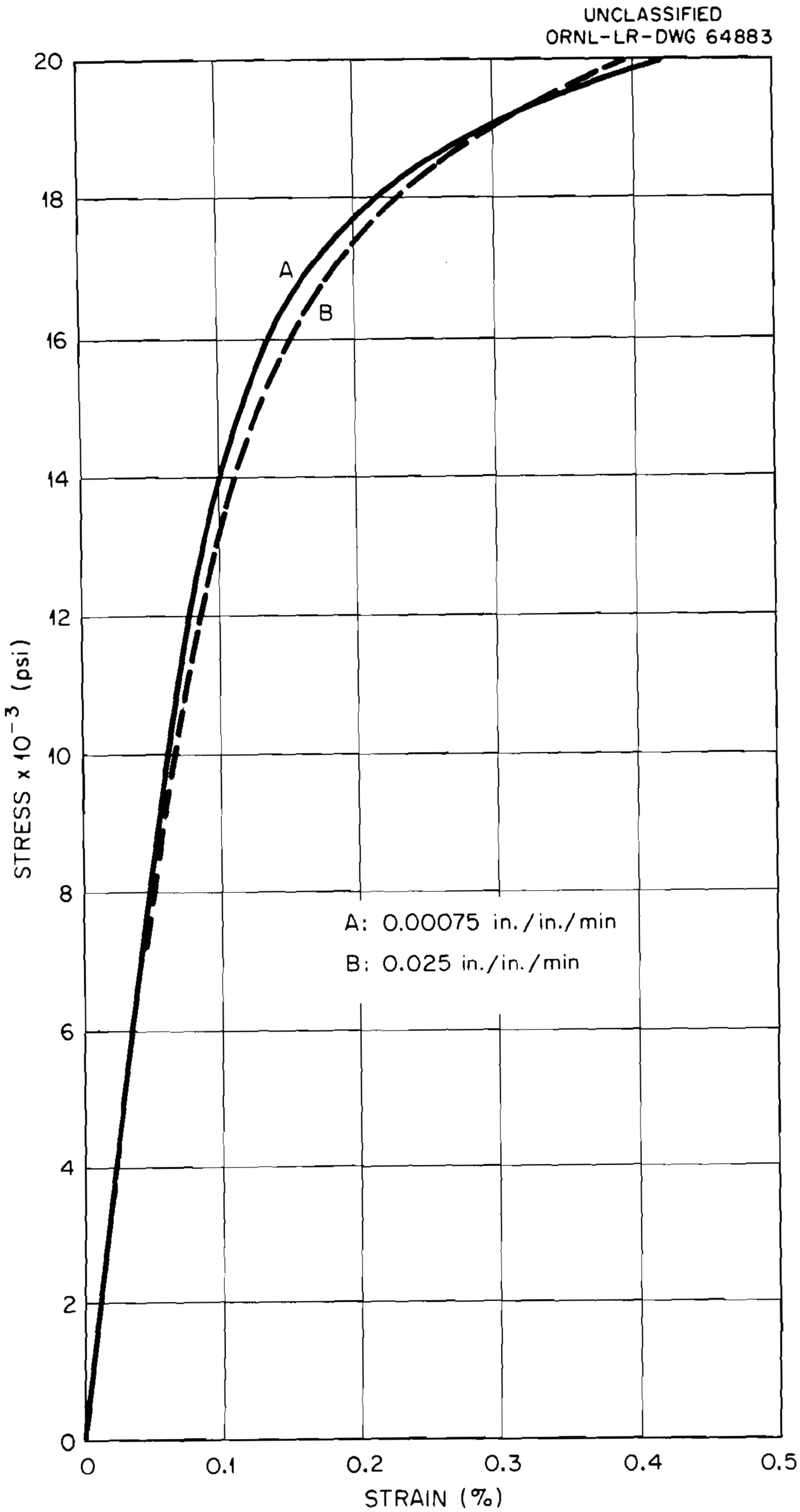

Fig. 3. Tensile Curves for Type 304 Stainless Steel Specimens at 1200°F — Heat 23999X.

UNCLASSIFIED
ORNL-LR-DWG 64884

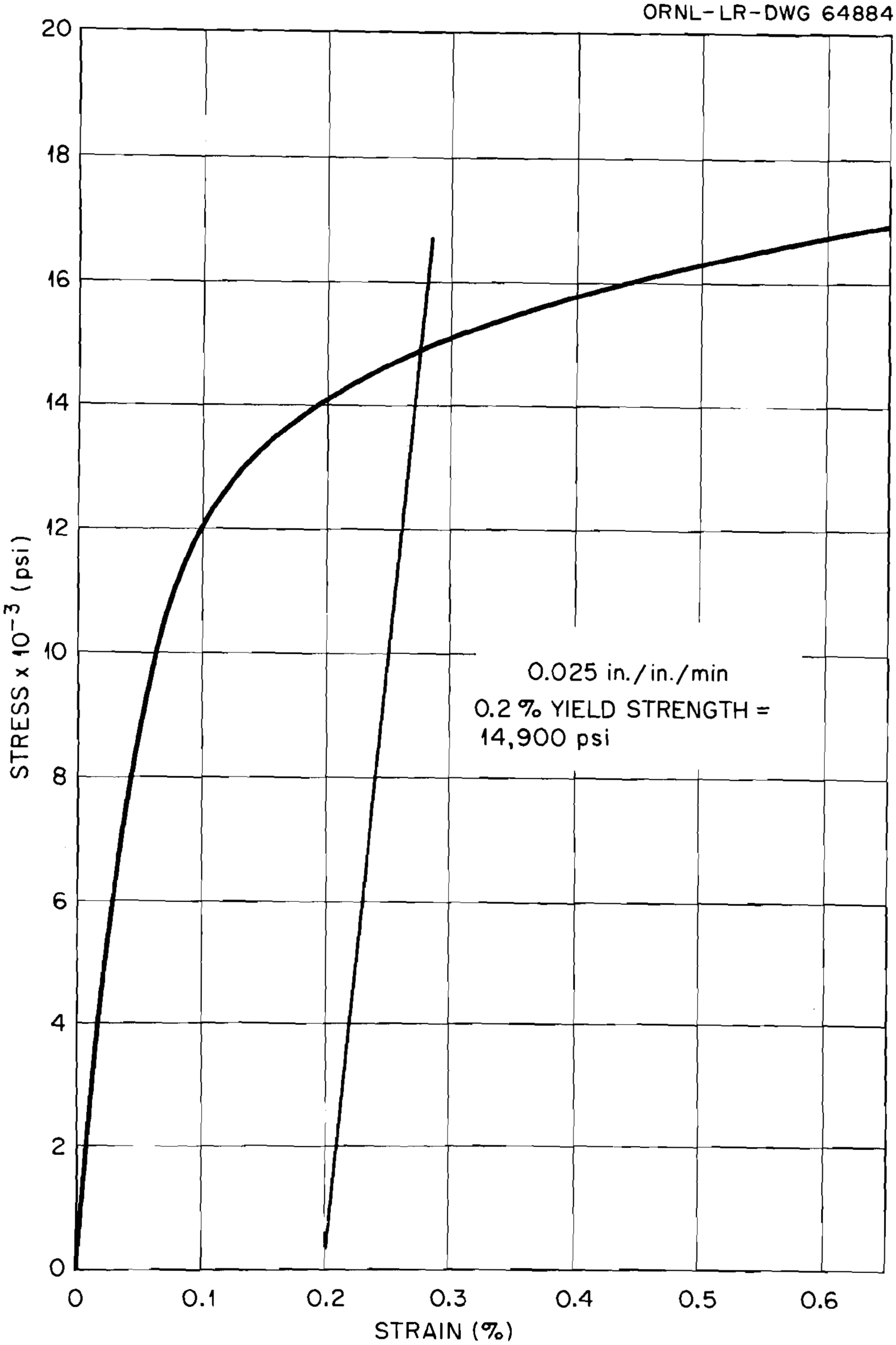

Fig. 4. Tensile Curve for Type 304 Stainless Steel Specimen at 1200°F – Heat 24555.

UNCLASSIFIED
PHOTO 56340

UNCLASSIFIED
Y-38418

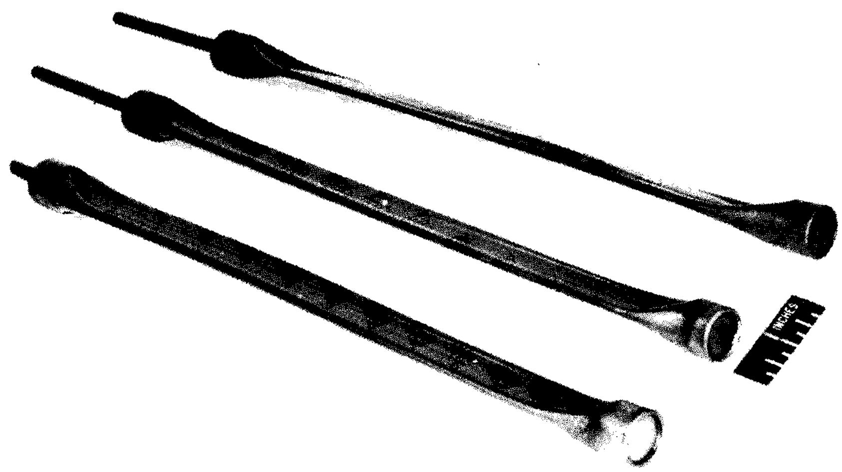

UNCLASSIFIED
Y-38417

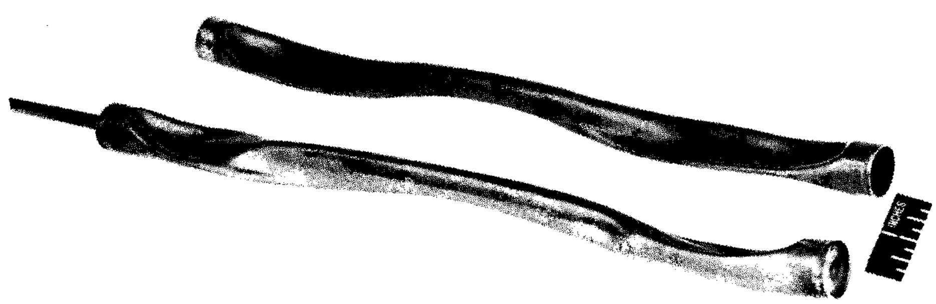

Fig. 5. Collapsed Tube Specimen for (a) Test Nos. 662, 656, and 663, with Wall-Thickness Variations of $\leq 5\%$, and (b) Test Nos. 664 and 640, with Wall-Thickness Variations of 10 to 13%.

DISCUSSION AND CONCLUSIONS

The attention given to the problem of the collapse of long, thin, circular, cylindrical shells by external pressure during the past hundred years has resulted in a number of theoretical and empirical solutions which form the basis for the design of such vessels.

The solution for elastic collapse of perfect tubes can be accomplished by using the von Mises[2] relationship:

$$\phi = \frac{(1 - \gamma^2)\, P_{cr} a}{E_r h_o} = \frac{1 - \gamma^2}{(n^2 - 1)\left(1 + \frac{n^2 \ell^2}{\pi^2 a^2}\right)^2} + \frac{h_o^2}{12a^2}\left(n^2 - 1 + \frac{2n^2 - 1 - \gamma}{1 + \frac{n^2 \ell^2}{\pi^2 a^2}}\right) , \qquad (1)$$

where

P_{cr} = the critical pressure for collapse (psi),
a = the mean radius of the tube (in.),
h_o = average or nominal wall thickness of tube (in.),
E_r = reduced modulus of elasticity (psi),
γ = Poisson's ratio 0.3,
ℓ = tube length between supports (in.),
n = number of lobes in collapsed tube.

The results of calculations using Eq. (1) are shown in Fig. 6, where ℓ/a is plotted vs ϕ. It is seen that a single curve for a given value of a/h_o is formed by combining portions of curves for integral values of n. The critical pressure for any given tube may be obtained through Fig. 6; however, the tube geometry necessary to resist a given pressure cannot be obtained without the use of unwieldy trial-and-error procedures. As a means of eliminating the necessity for such procedures the following graphical solution was developed.

---

[2]R. von Mises, Z. Ver. deut. Ingr. (VDI z.) 58, 750 (1914).

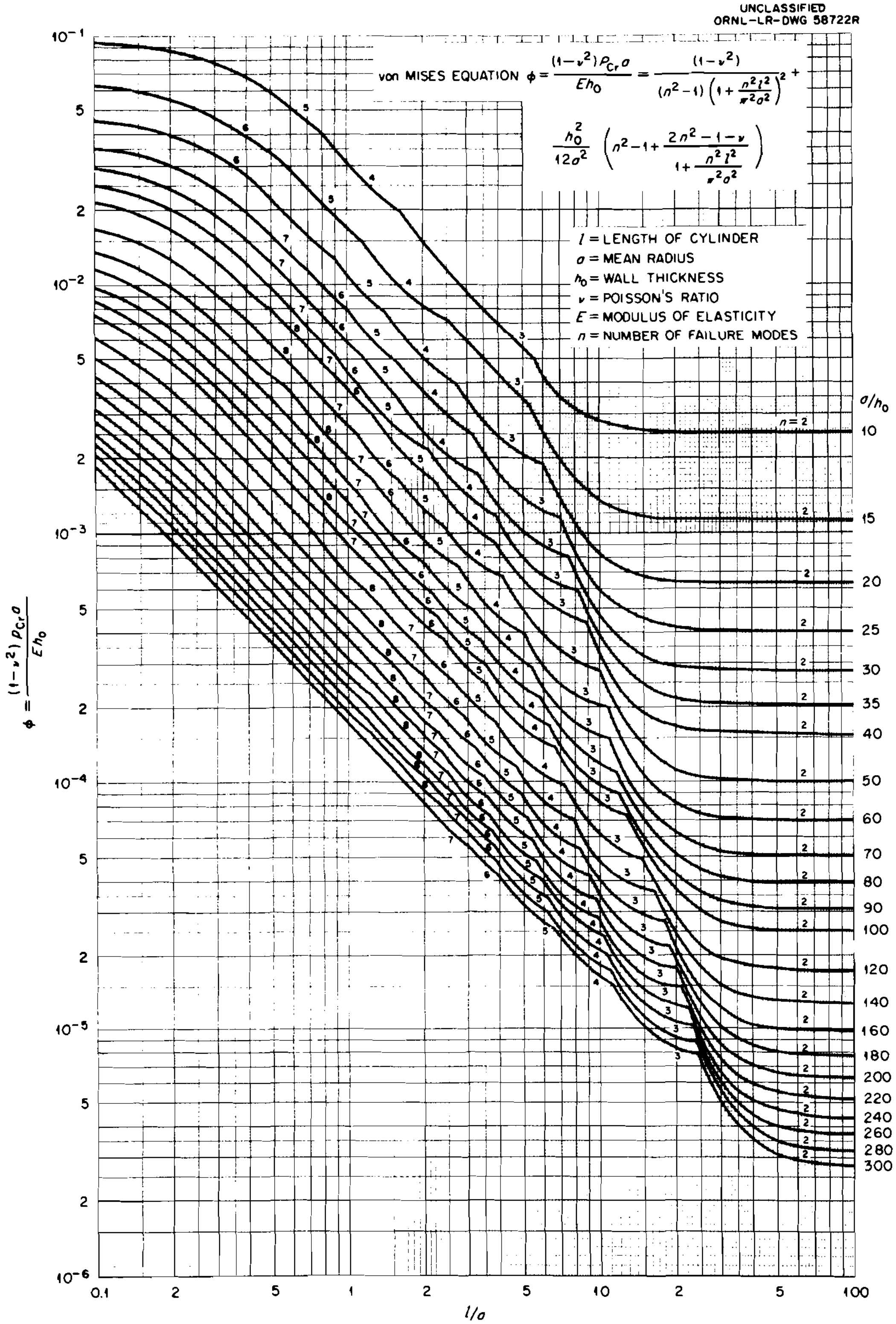

Fig. 6. Master Curve for Critical External Pressure To Collapse Cylindrical Vessels.

Equation (1) may be modified to

$$\left(P_{cr}\right)_{\ell/a} = (f) \frac{E_r}{4(1 - \gamma^2)} \left(\frac{h_o}{a}\right)^3 \quad , \tag{2}$$

where (f) = the ratio of Φ for a given ℓ/a and Φ for an infinite-length tube, obtained from Fig. 6. It is observed in Eq. (1) and more clearly shown in Eq. (2) that the critical pressure is a linear function of the reduced modulus for fixed values of ℓ/a and a/h_o.

The stress distribution across the tube wall varies depending on whether the deformation is elastic or plastic. The average stress, however, is given by

$$\sigma_\theta = P \frac{a}{h_o} \quad , \tag{3}$$

where σ_θ = stress in tangential direction (psi) and P = pressure (psi). By combining Eqs. (2) and (3)

$$\sigma_{\theta_{cr}} = KE_r \quad , \tag{4}$$

where

$$K = \frac{(f)}{4(1 - \gamma^2)} \left(\frac{h_o}{a}\right)^2 \quad .$$

By substituting values of (f) and a/h_o in Eq. (4), a series of straight parallel lines may be generated on a logarithmic plot of stress vs reduced modulus. Since the designer is primarily concerned with the tube geometry necessary to resist a particular pressure, Eq. (3) is used to construct straight parallel isobars superimposed on the previously obtained plot. Each isobar intersects the constant (f) and a/h_o lines at a stress satisfying Eq. (3). A plot as described above is shown in Fig. 7 for infinite-length tubes [(f) = 1].

The addition of a material line to Fig. 7 will now yield conditions of stability and instability for tubes under external pressure. This material line should ideally be obtained from compression tests; however, the use of tensile data to the strains of interest will not introduce significant error.

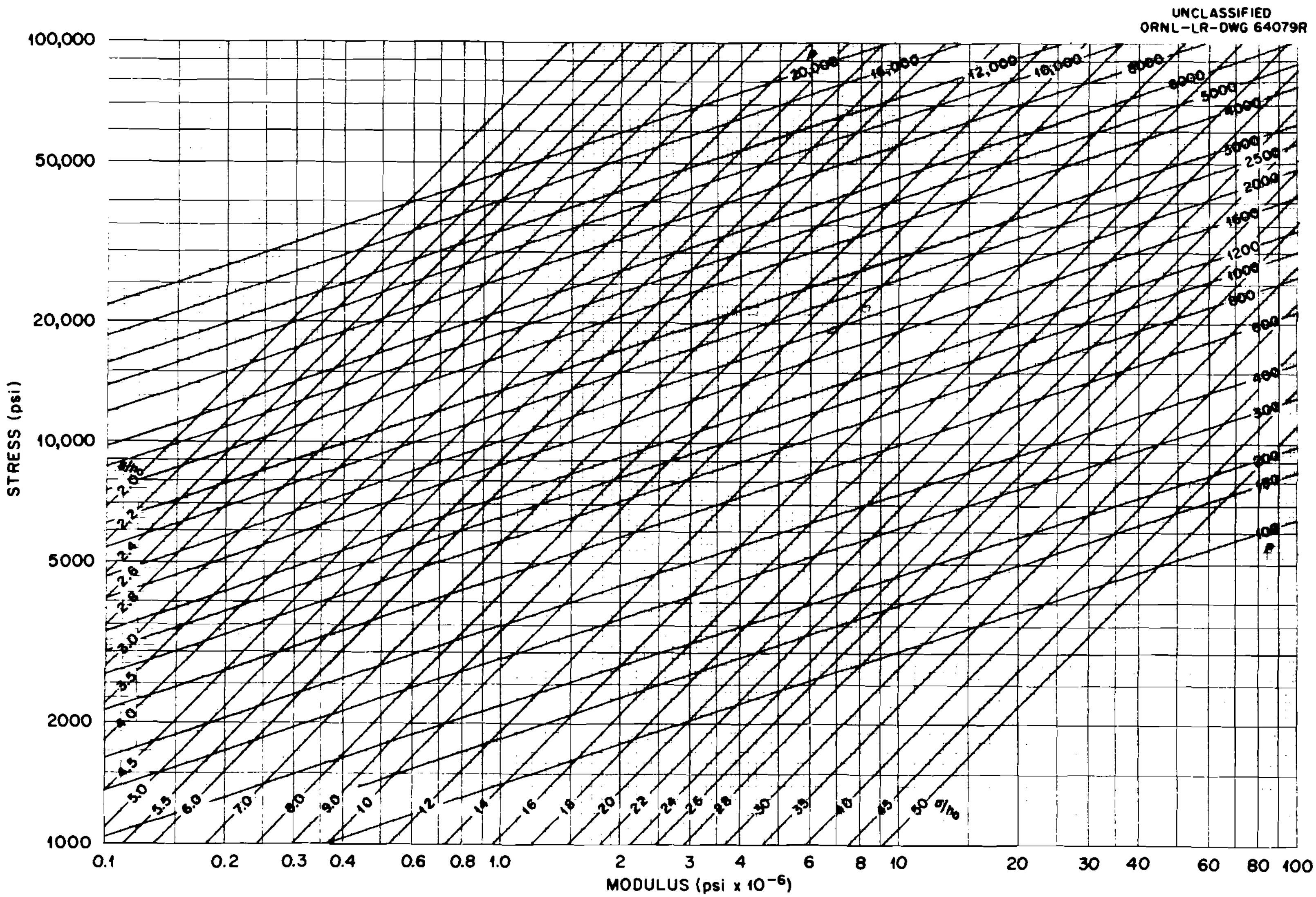

Fig. 7. Logarithmic Plot of Geometric Factors for Infinite-Length Tubes.

The reduced modulus, defined by von Karman,[3] considers the stress redistribution due to yielding:

$$E_r = \frac{4EE_\sigma}{\left(E^{\frac{1}{2}} + E_\sigma^{\frac{1}{2}}\right)^2} \quad , \tag{5}$$

where E_r = reduced modulus (psi), E = Young's modulus (psi), and E_σ = tangent modulus (psi). The material lines, represented as a logarithmic plot of stress vs reduced modulus, are given in Figs. 8 and 9 for two heats of type 304 stainless steel used in this investigation. Figures 10 and 11 show these material lines superimposed on the geometric plots previously developed.

Intersections of a/h_o lines with isobars which occur on, above, or to the right of the material lines in Figs. 10 and 11 are situations which will result in instantaneous collapse. Combinations of a/h_o and pressure lines intersecting below the material lines will not result in instantaneous collapse. Verification of these results with the experiments for the two heats of material is given in Fig. 12.

It should be recognized that the effect of increasing temperature is a lowering of the elastic limit of the material and that inelastic collapse becomes possible at lower pressures. The critical stress necessary for collapse in all tests shown in Fig. 12 was greater than the elastic limit of the material. Thus, without the graphical solution as shown in Figs. 10 and 11, it would be necessary to design to the elastic limit and accept the existence of an unknown safety factor or to use a tedious trial-and-error solution to obtain exact answers.

The use of the graphic solution in Figs. 10 and 11 allows direct solution of the tube collapse problem with any desired safety factor. The plots shown are applicable for infinite-length tubes only; for tubes with smaller ℓ/a ratios, (f) must be determined from Fig. 6. The direct

---

[3]Th. von Karman, Forsch. Gebiete Inenieurw. VDI — Forschungsheft 81, 20 (1910).

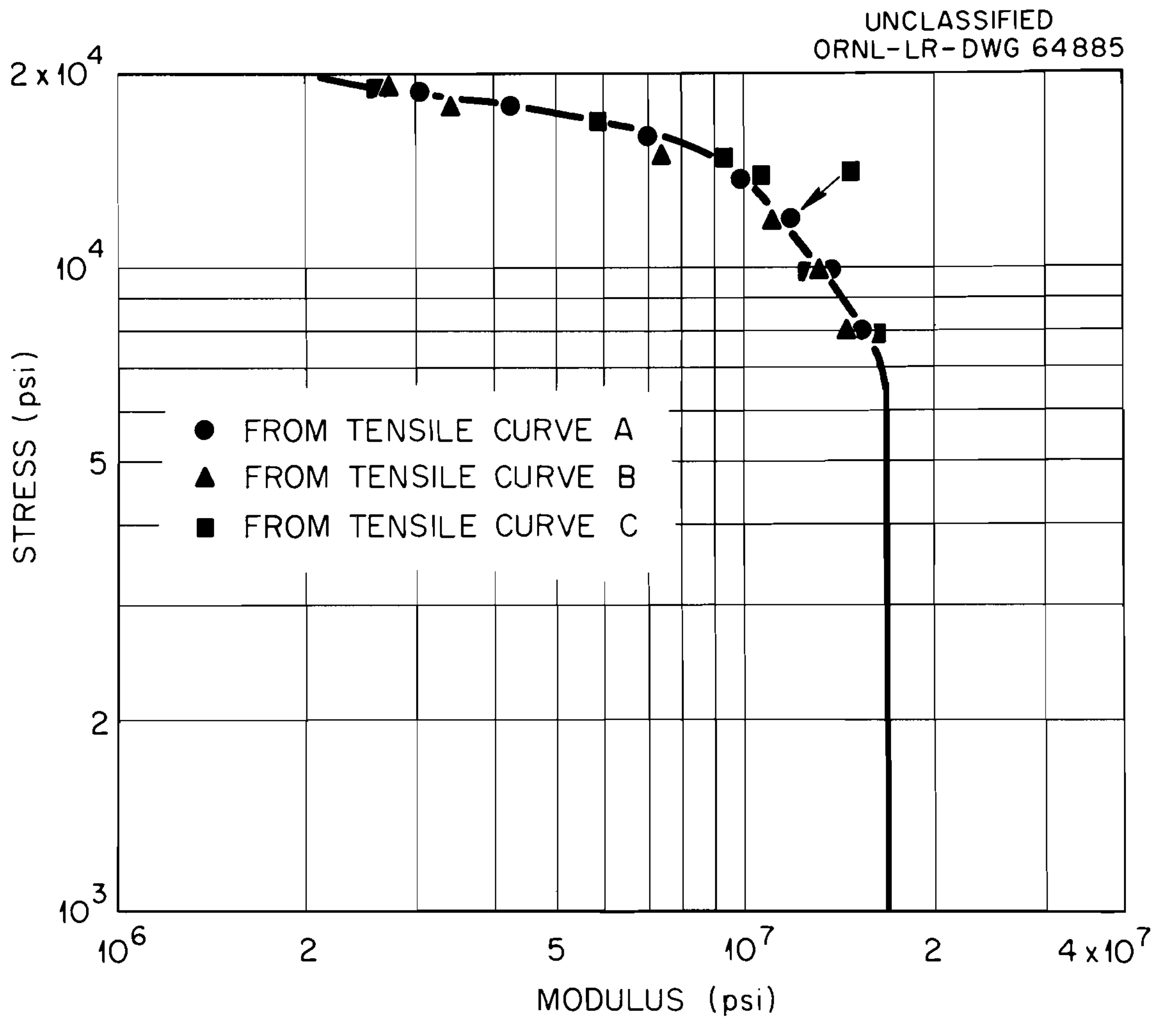

Fig. 8. Logarithmic Plot of Stress vs Reduced Modulus for Type 304 Stainless Steel Specimen at 1200°F — Heat 23999X.

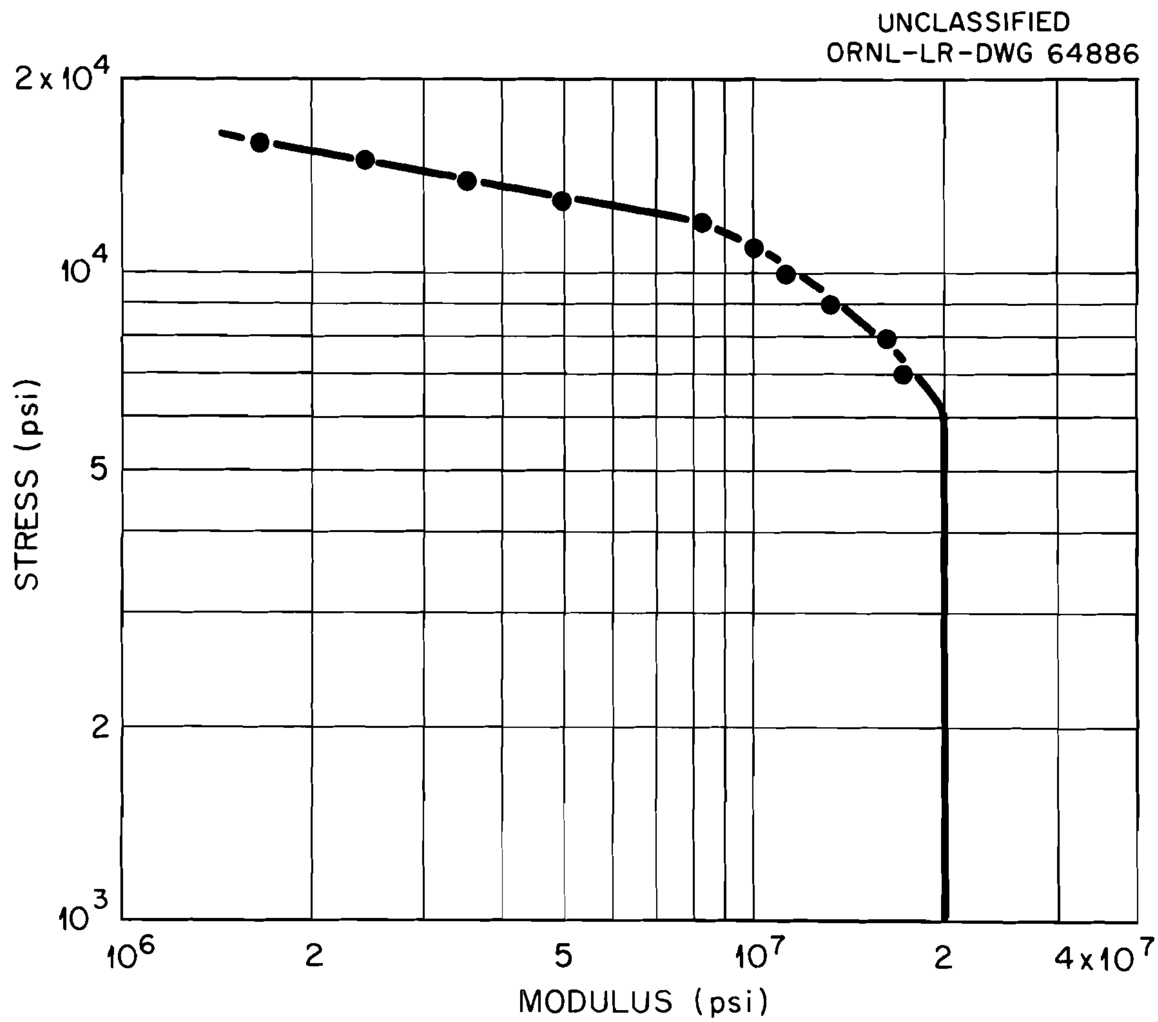

Fig. 9. Logarithmic Plot of Stress vs Reduced Modulus for Type 304 Stainless Steel Specimen at 1200°F — Heat 24555.

UNCLASSIFIED
ORNL-LR-DWG 64887R

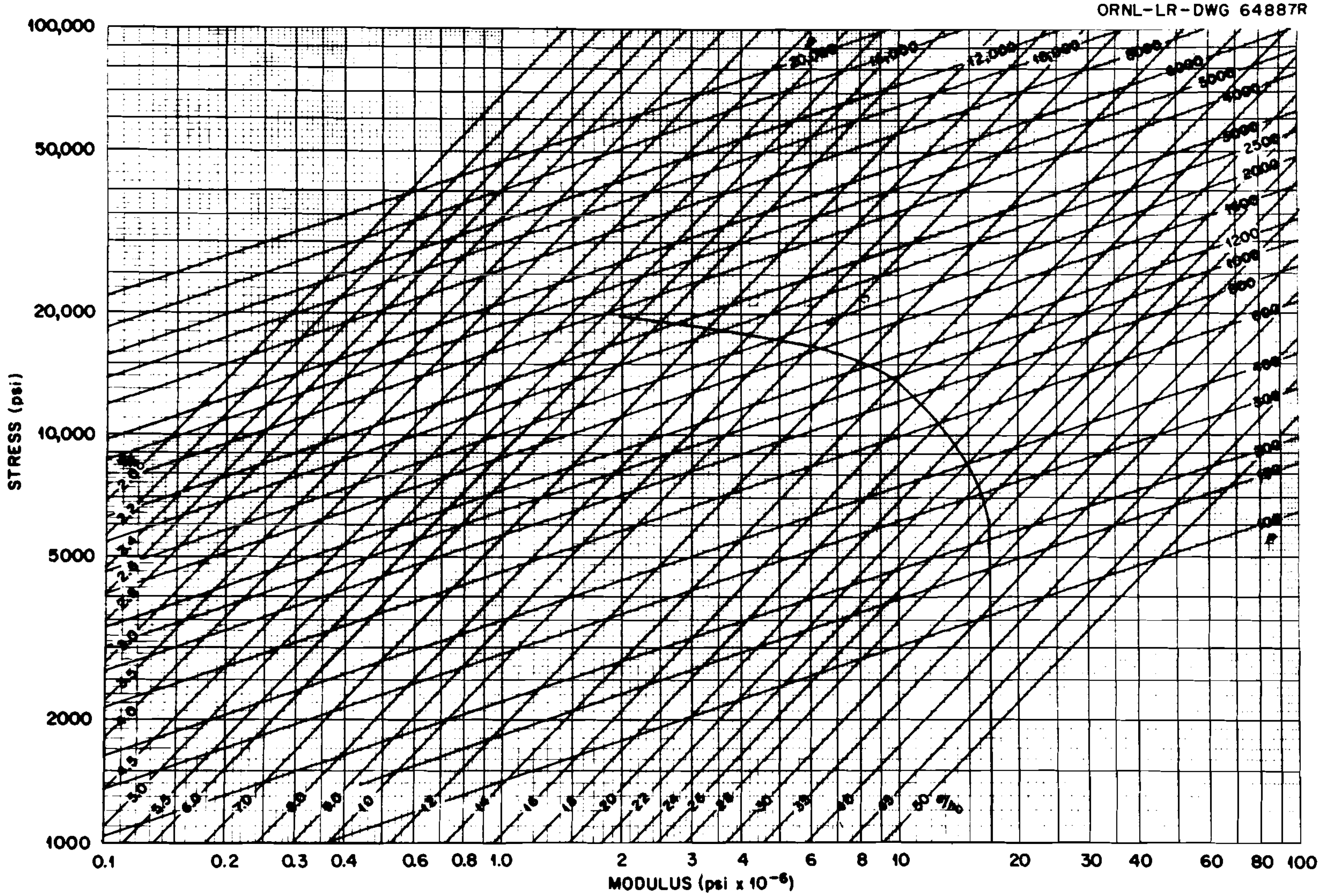

Fig. 10. Graphical Solution for Tube Collapse — Heat 23999X.

UNCLASSIFIED
ORNL-LR-DWG 64888R

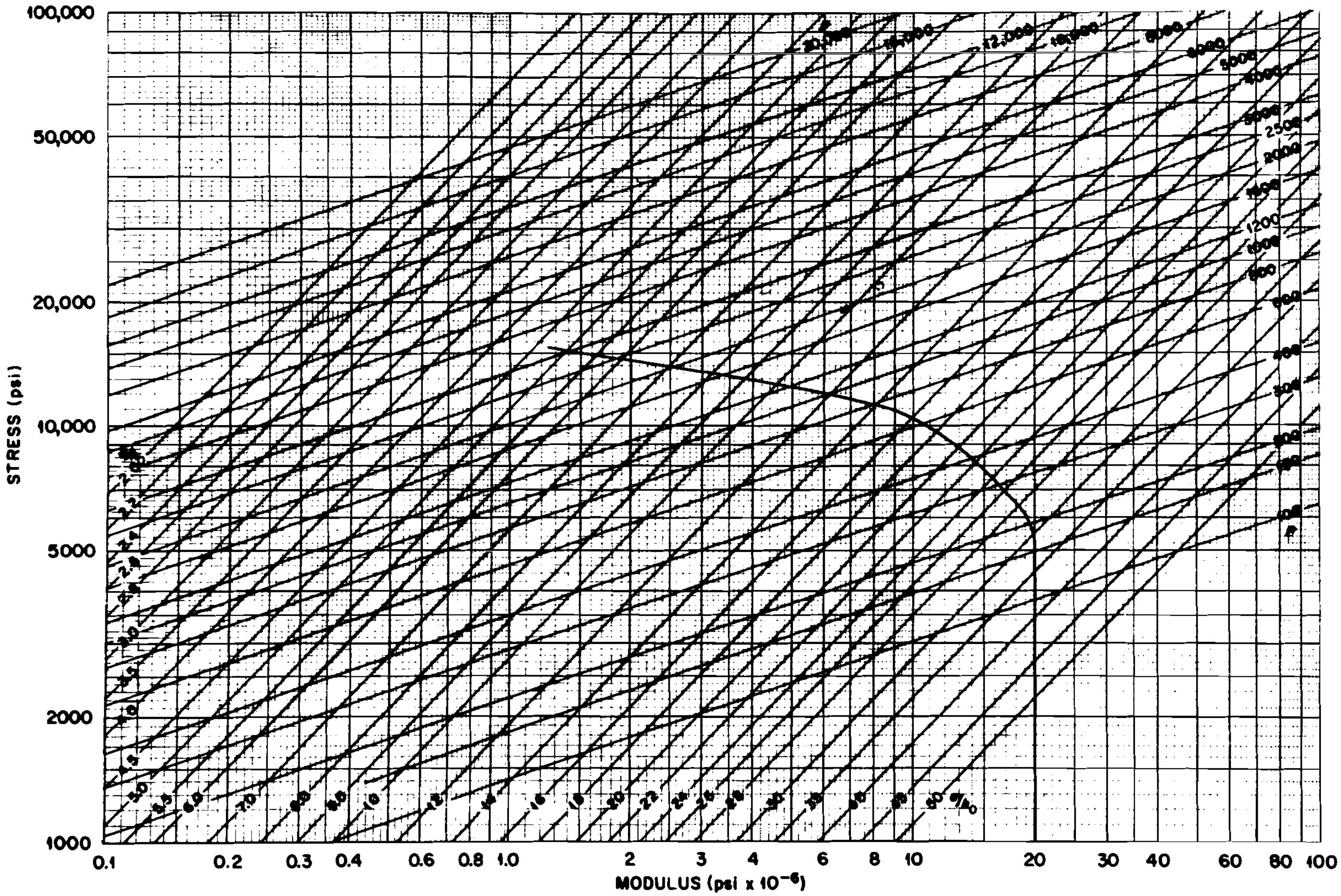

Fig. 11. Graphical Solution for Tube Collapse — Heat 24555.

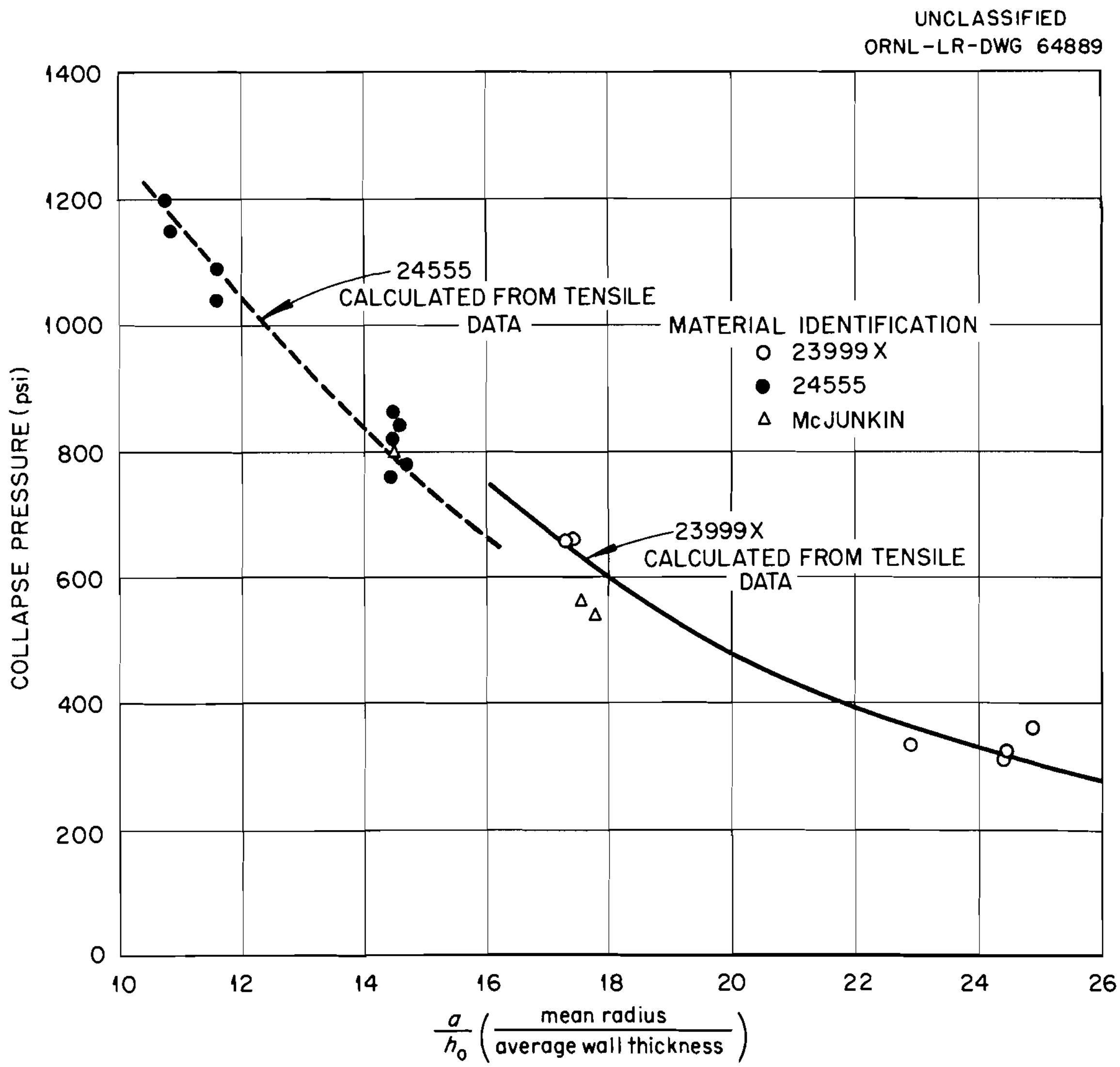

Fig. 12. Instantaneous Collapse Pressure vs a/h_o. Curves calculated from tensile data.

proportionality of (f) and critical pressure is no longer valid for inelastic collapse since the reduced modulus varies with stress. The factor (f) for a given ℓ/a ratio also varies slightly with the a/h_o ratio, and therefore the same (f) cannot be used to shift all the a/h_o lines in Figs. 10 and 11. A method which may be used to determine the effect of reducing the ℓ/a ratio is to make an appropriate shift of the material line to the right for a given ℓ/a ratio.

For design purposes the minimum expected material properties of type 304 stainless steel at 1200°F should be used. The graphic solution based on these minimum values is shown in Fig. 13 and includes the effect of lowering the ℓ/a ratio. This was done by shifting the material line to the right through the use of Fig. 6.

This solution does not imply that tubes under a pressure less than the critical pressure for prolonged periods of time will not collapse, since creep is important at 1200°F. In fact, time-dependent behavior may be important even under rapid increases in pressure for certain materials and temperatures. For this particular case of type 304 stainless steel at 1200°F, the tensile data were unaffected by strain-rate variations in the testing range, and time dependency is therefore felt to be negligible in these results.

Selection of a suitable safety factor is dependent upon several criteria, for example, anticipated perfection of the tube, minimum expected strength of the material, and cost of fabrication and operation vs cost of failure and replacement. The major imperfections in tubing, ovality, and wall-thickness variation will now be evaluated.

The most severe reduction in collapse pressure results from tube ovality or out-of-roundness. Timoshenko[4] has shown that the maximum stress acting on the tube wall of an oval specimen is given by

$$\sigma_{max} = \frac{Pa}{h_o} + \frac{6Pa}{h_o^2} \frac{w_o}{1 - \frac{P}{P_{cr}}} , \qquad (6)$$

---

[4] S. Timoshenko, Theory of Elastic Stability, McGraw-Hill, New York, 1936.

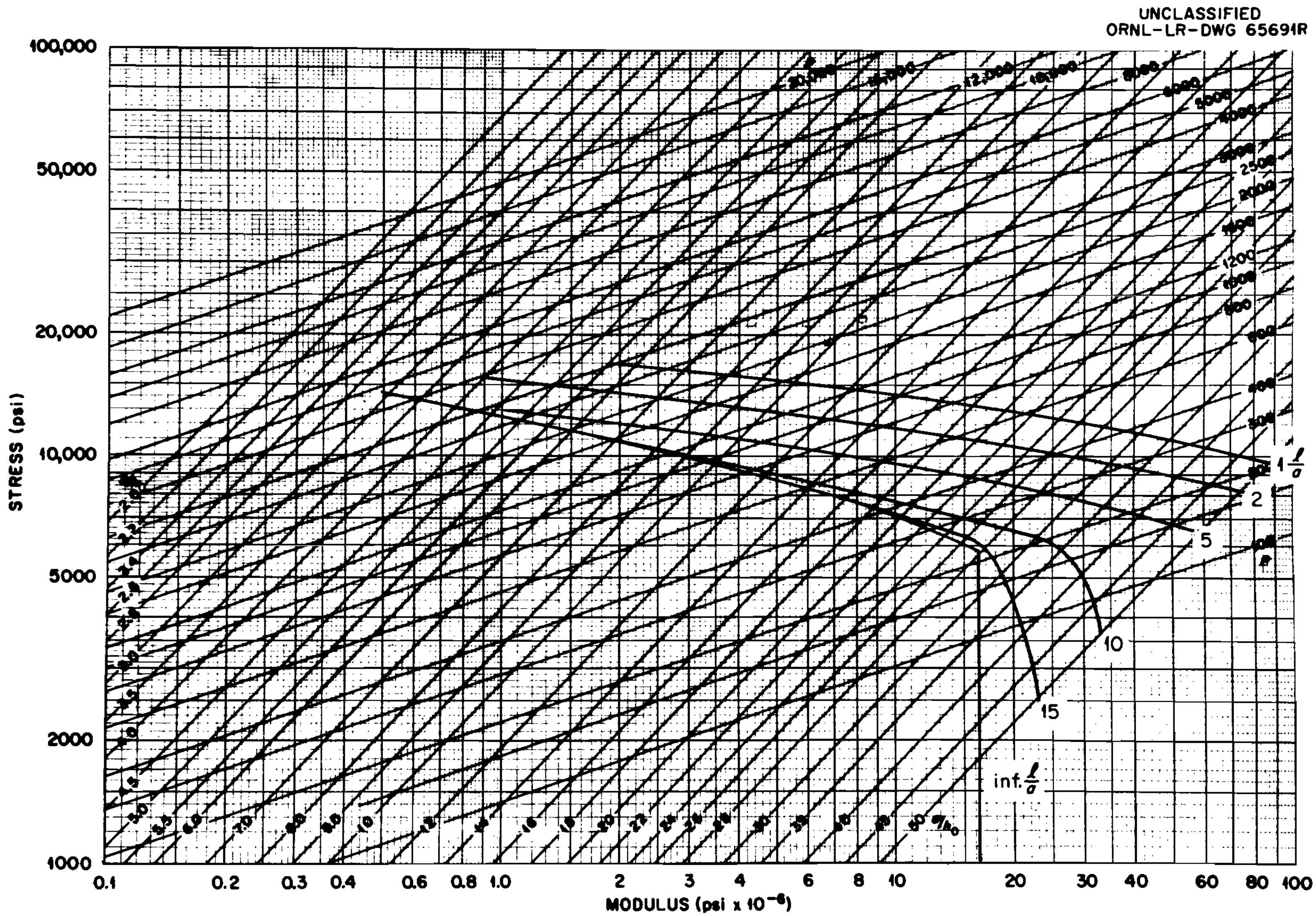

Fig. 13. Graphical Solution for Collapse Problem for Tubes of Less Than Infinite Length.

where

σ_{max} = maximum stress in tube wall (psi),

w_o = maximum initial deflection of tube

= 1/4 (OD_{max} - OD_{min}) (in.),

P_{cr} = critical pressure for collapse of perfect tube (psi).

In his discussion of the above formula Timoshenko indicated that the maximum stress which could be resisted is the yield stress of the material. With materials which do not exhibit a definite yield point, some uncertainty exists as to the proper value for σ_{max}. It was found that setting σ_{max} equal to the value of the 0.2%-offset yield strength obtained from the tensile curve of the material resulted in a good correlation with experimental results. Equation (6) may be solved for the ratio P_o/P_{cr} as follows:

$$\frac{P_o}{P_{cr}} = R = \frac{\left(\frac{\sigma_{max}}{\sigma_{cr}} + 1 + 6\frac{w_o}{h_o}\right) - \left[\left(\frac{\sigma_{max}}{\sigma_{cr}} - 1 - 6\frac{w_o}{h_o}\right)^2 + 24\frac{\sigma_{max}}{\sigma_{cr}}\frac{w_o}{h_o}\right]^{\frac{1}{2}}}{2} , \quad (7)$$

where

P_o = pressure for collapse of the oval tube (psi),

P_{cr} = pressure for collapse of a perfect tube of same a/h_o (psi),

σ_{max} = 0.2%-offset yield strength of material (psi),

σ_{cr} = critical stress for collapse of a perfect tube of same a/h_o (psi).

The correlation of the foregoing equation and experimental values is shown in Fig. 14. It should be noted that the effect of ovality varies with w_o/h_o and with σ_{max}/σ_{cr}, the latter varying with the material.

Wall-thickness variation will also cause a reduction in the collapse pressure; however, this reduction is relatively small in comparison with that of ovality. Ellington[5] in considering this problem proposed the

[5]J. P. Ellington, The Critical Pressure of a Tube with an Eccentric Bore, DEG-43(R) (1960).

UNCLASSIFIED
ORNL-LR-DWG 64890

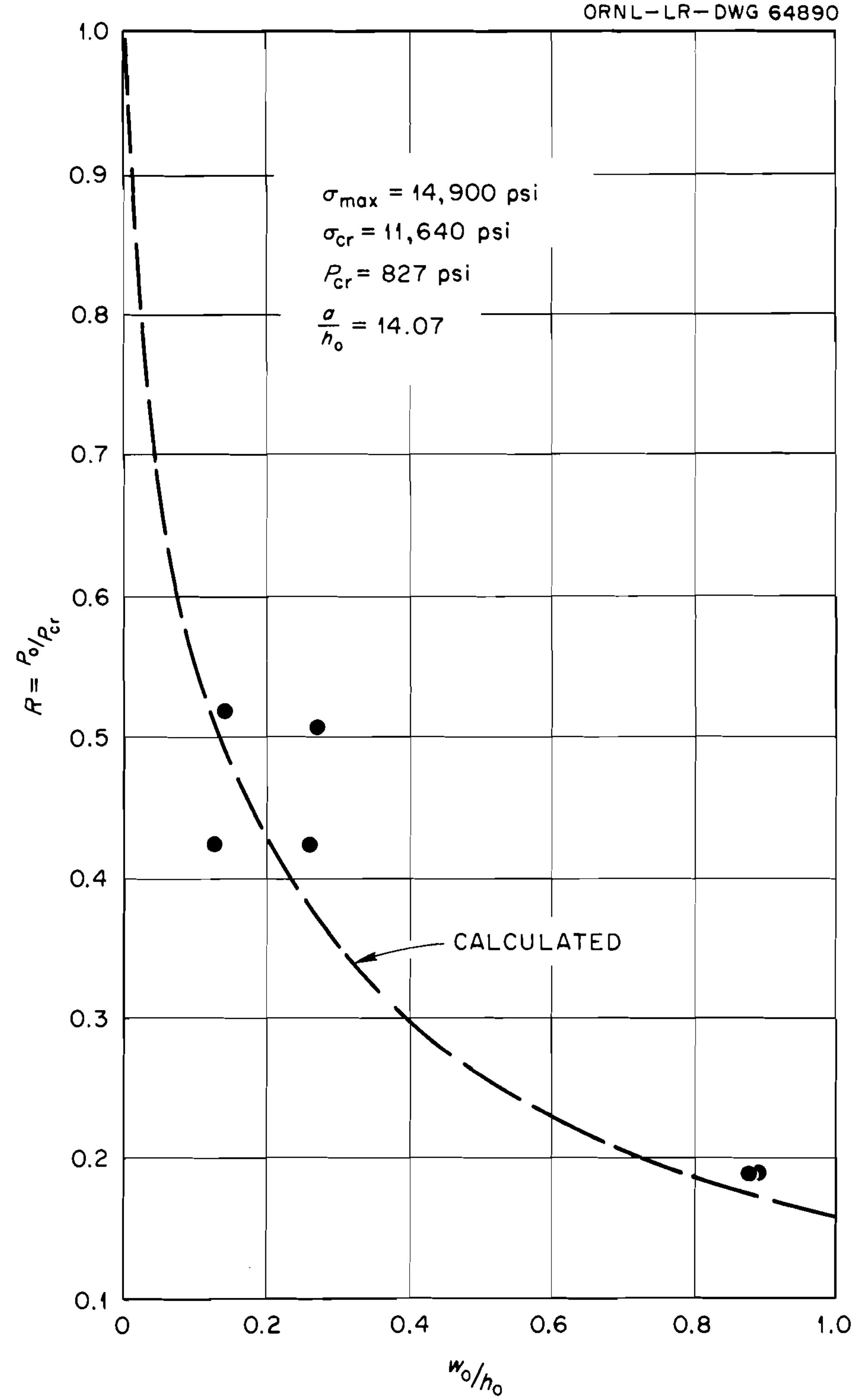

Fig. 14. Plot Showing Effect of Ovality on Instantaneous Collapse Pressure.

following relationship:

$$\frac{P_v}{P_{cr}} = \frac{1}{3}\left[9 - 6\ (1 + 3v^2)^{\frac{1}{2}}\right] \quad , \tag{8}$$

where v = minimum wall-thickness variation $\left(\frac{h_o - h_{min}}{h_o}\right)$ and P_v = pressure for collapse of tubes having wall-thickness variations v. It is interesting to note that this relationship is independent of a/h_o and ℓ/a. A comparison of Ellington's relationship with the test results is given in Fig. 15. It can be seen that a 10% variation in wall thickness produces only a 3% reduction of the critical pressure, an effect which is considered to be insignificant since most vendors can readily produce tubing within such a tolerance and since the scatter in the experimental results exceeds 3%.

The foregoing discussion serves to demonstrate how the critical pressure for instantaneous collapse may be obtained and what the effects of tube imperfections are. Therefore, with the minimum expected strength of the material and the expected imperfections known, it is possible to design with any desired confidence factor tubes to resist collapse.

Time-Dependent Collapse

Although no experimental work has been performed on time-dependent collapse, it is felt that this phenomenon warrants discussion.

An exact solution of the creep-buckling problem is limited by the lack of proper and exact generalizations of the tension-creep stress-strain relations to multiaxial stress with changing principal stress directions. Several tentative solutions have been proposed[6,7] which are approximate because of the many necessary simplifying assumptions made.

---

[6]N. J. Hoff, W. E. Jahsman, and W. Nachbar, A Study of Creep Collapse of a Long Cylinder Under Uniform External Pressure, LSMD-2360 (March 28, 1958).

[7]J. P. Ellington, Creep Collapse of Tubes Under External Pressure, DEG-162(R) (1960).

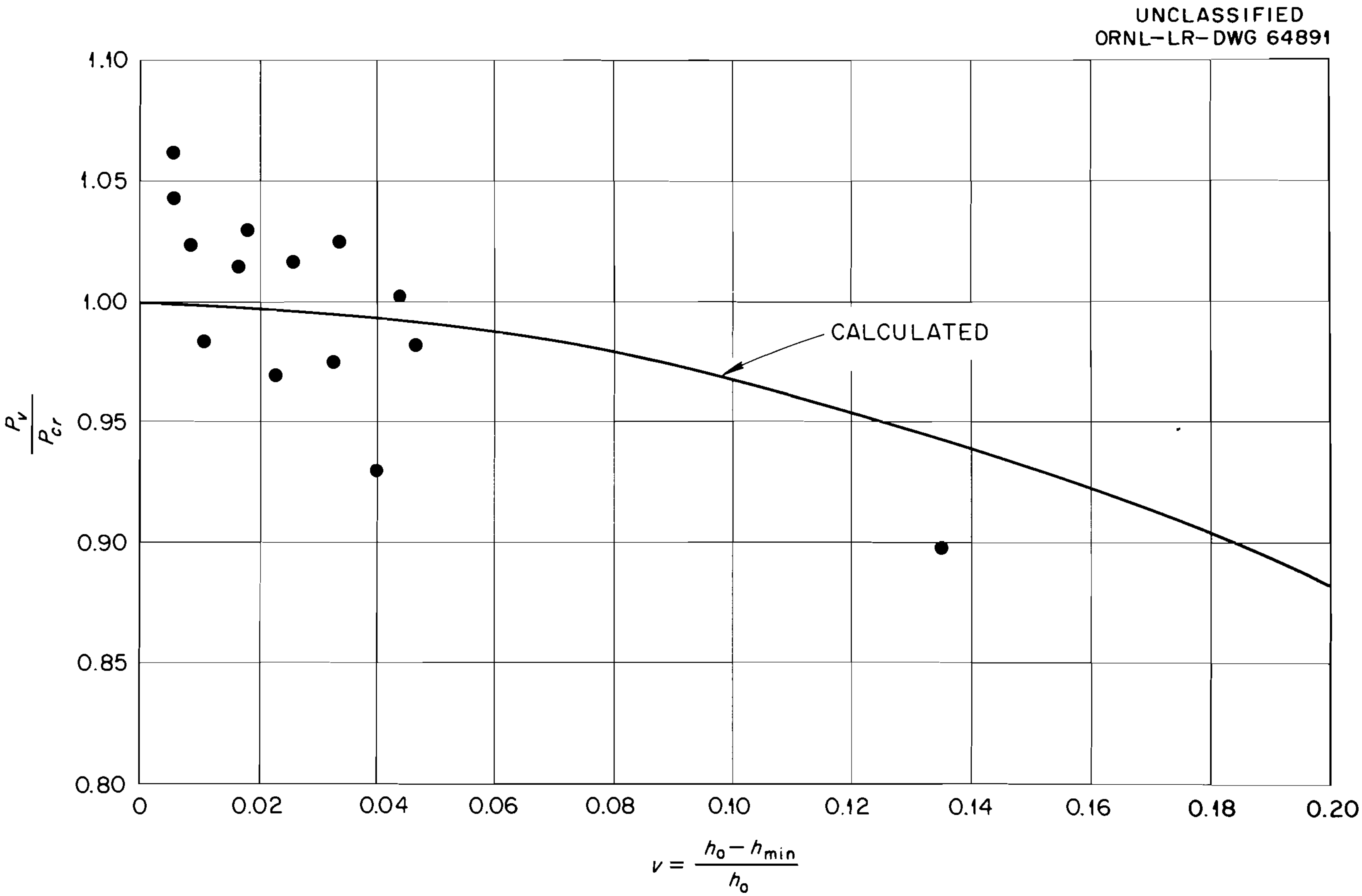

Fig. 15. Plot Showing Effect of Wall-Thickness Variation on Instantaneous Collapse Pressure.

An approximate solution which may be more easily handled than those referred to above can be obtained by using an analysis of the "deformation theory" type. Such an approach to inelastic buckling assumes that total strain at a given time is described by the equation resulting from principal strains being always proportional to principal stresses with no rotation of the principal axis occurring. When the lateral deflection of the tube wall, or buckling, begins to occur because of increasing stresses, the magnitude of this deflection is computed as though the new increased stress had been applied throughout the entire loading period. This method should then provide a lower limit to the inelastic buckling load of members with limited geometric imperfections. Application of the inelastic-buckling solution to pin-jointed columns has demonstrated the conservatism of such a prediction of time to failure.

Inelastic-buckling solutions for tube collapse are obtained by replacing the reduced modulus in the previously developed equations with an effective modulus. Two such effective moduli ($E_{\dot{\epsilon}}$ and E_t) have been proposed for solution of column buckling:

$$E_{\dot{\epsilon}} = \left(\frac{\partial \sigma}{\partial \epsilon}\right)_{\dot{\epsilon}} \quad , \qquad (9)$$

which was proposed by Robotnov[8] and defined as the tangent slope of the constant strain-rate stress vs strain curve; and

$$E_t = \left(\frac{\partial \sigma}{\partial \epsilon}\right)_t \quad , \qquad (10)$$

proposed by Shanley[9] and defined as the tangent slope of the isochronous stress-strain curves.

Expressions for both moduli may be obtained from the creep equation

$$\epsilon_c = \left(\frac{\sigma}{A}\right)^{\alpha} t^m \quad , \qquad (11)$$

where ϵ_c = creep strain (in./in.), t = time (hr), and A, α, m = material

[8] G. N. Robotnov and S. A. Shesterikov, J. Mech. and Phys. Solids 6, 27 (1957).

[9] R. F. Shanley, "Principles of Creep Buckling," Chap. 19 in Weight-Strength Analysis of Aircraft Structures, McGraw-Hill, New York, 1952.

constants, and from the total strain equation

$$\epsilon_t = \epsilon_c + \frac{\sigma}{E} \quad , \tag{12}$$

where ϵ_t = total strain. The resulting expressions are then

$$E_{\stackrel{o}{\epsilon}} = \left[\frac{\alpha\epsilon_c}{(1 - m)\sigma} + \frac{1}{E}\right]^{-1} \tag{13}$$

and

$$E_t = \left(\frac{\alpha\epsilon_c}{\sigma} + \frac{1}{E}\right)^{-1} \quad . \tag{14}$$

It should be noted that if m were to become equal to 1, $E_{\stackrel{o}{\epsilon}}$ would go to zero for all values of stress regardless of the material strength. Since it is not uncommon that m = 1 for many materials, it is felt that the Robotnov effective modulus is not suitable for use in tube-buckling equations. The stress-strain relationships to be considered in tube collapse are those occurring in the tangential direction, and it has been shown[10] that for capped end tubes

$$\epsilon_{c_\theta} = \frac{3}{4}\epsilon_c \quad , \tag{15}$$

where ϵ_{c_θ} = tangential creep strain under tangential stress σ_θ, and ϵ_c = uniaxial creep strain under a uniaxial stress equal to σ_θ.

Substituting in Eq. (14) yields

$$E_t = \left(\frac{\alpha\epsilon_{c_\theta}}{\sigma_\theta} + \frac{1}{E}\right)^{-1} \tag{16}$$

or

$$E_t = \left(\frac{3}{4}\frac{\alpha\epsilon_c}{\sigma_\theta} + \frac{1}{E}\right)^{-1} \quad . \tag{17}$$

---

[10] C. R. Kennedy, W. O. Harms, and D. A. Douglas, Trans. Am. Soc. Mech. Engrs. J. Basic Engr. **81** (Series D), 599 (1959).

The resulting tube collapse relationship from Eq. (2) is then

$$P_{cr} = (f) \frac{E_t}{4(1 - \gamma^2)} \left(\frac{h_o}{a}\right)^3 \tag{18}$$

or

$$P = P_{cr} \frac{E_t}{E_r} \ . \tag{19}$$

As was previously pointed out, Eq. (19) does not yield an exact solution for the critical time of collapse but yields, instead, the critical time for the loss of stability in the classical sense. After the critical time has elapsed, any small disturbance applied to the tube should result in deflections which increase with time. Collapse may then be expected at some time greater than the critical time for loss of stability calculated by Eq. (19).

A simple relationship or proportionality will possibly exist for critical time vs actual collapse time but it must be determined experimentally. Until such experiments have been performed, the conservative prediction in Eq. (19) should be used.

An important result of the above analysis is that the previously developed graphical solution may again be utilized. The substitution of a material curve of E_t vs σ_θ corresponding to the design lifetime of the vessel for the material curve of E_r vs σ will produce the solution of Eq. (18).

CONCLUSIONS

The following conclusions on tube collapse at 1200°F for type 304 stainless steel have been reached:

1. The use of the von Karman reduced modulus in collapse equations adequately accounts for inelastic behavior of the material under rapidly applied loading.

2. The graphical method developed, which superimposes material behavior on tube geometry, allows the application of known safety factors in design to resist instantaneous collapse.

3. The effect of ovality, a serious imperfection which greatly reduces the pressure for instantaneous collapse, can be predicted.

4. The reduction of collapse pressure due to wall-thickness variations within normal manufacturing tolerances may be neglected.

5. A critical time, after which collapse may occur, exists for a tube under an external pressure less than the critical pressure for instantaneous collapse.

ACKNOWLEDGMENTS

The authors wish to thank F. L. Beeler and C. W. Walker for their assistance in the experimental program.

DISTRIBUTION

1–2. Central Research Library
3. ORNL – Y-12 Technical Library Document Reference Section
4–6. Laboratory Records
7. Laboratory Records, ORNL RC
8. G. M. Adamson, Jr.
9. E. E. Barton
10. R. E. Clausing
11. J. H. Coobs
12. J. M. Corum
13. J. E. Cunningham
14. J. H. DeVan
15. C. W. Dollins
16. D. A. Douglas, Jr.
17. H. G. Duggan
18. J. H Frye, Jr.
19. B. L. Greenstreet
20. J. P. Hammond
21. W. O. Harms
22. D. M. Hewette II
23–25. M. R. Hill
26–31. C. R. Kennedy
32. C. F. Leitten, Jr.
33. A. L. Lotts
34. H. G. MacPherson
35. W. D. Manly
36. W. R. Martin
37. H. E. McCoy, Jr.
38. P. Patriarca
39. M. J. Skinner
40. G. M. Slaughter
41. R. L. Stephenson
42. R. W. Swindeman
43. A. Taboada
44. W. C. Thurber
45–50. J. T. Venard
51. J. R. Weir, Jr.
52. J. W. Woods
53. A. F. Zulliger
54–68. Division of Technical Information Extension (DTIE)
69. Research and Development Division (ORO)